THE JOURNAL OF PHYSICAL CHEMISTRY B

Article

pubs.acs.org/JPCB

Circular Dichroism and Optical Rotation of Lactamide and 2-Aminopropanol in Aqueous Solution

Anna Pikulska,[†] Kathrin H. Hopmann,[‡] Julien Bloino,[¶,§] and Magdalena Pecul*,[†]

[†]Faculty of Chemistry, University of Warsaw, Pasteura 1, 02-093 Warszawa, Poland

[‡]Centre for Theoretical and Computational Chemistry, Department of Chemistry, University of Tromsø, N-9037 Tromsø, Norway

[¶]Consiglio Nazionale delle Ricerche, Istituto di Chimica dei Composti Organometallici (ICCOM-CNR), UOS di Pisa, Area della Ricerca CNR, via G. Moruzzi 1, I-56124 Pisa, Italy

[§]Scuola Normale Superiore, Piazza dei Cavalieri 7, I-56126 Pisa, Italy

ABSTRACT: The performance of implicit and explicit solvent models (polarizable continuum model (PCM) and microsolvation with positions of water molecules obtained either from molecular dynamics (MD) simulations or quantum mechanical geometry optimization) for calculations of electronic circular dichroism (CD) and optical rotation (OR) is examined for two polar and flexible molecules: lactamide and 2-aminopropanol. The vibrational structure of the CD spectrum is modeled for lactamide. The results are compared with the newly obtained experimental data. The signs of the bands are correctly reproduced using all three methods under investigation and the CAM-B3LYP functional for the CD spectrum of lactamide, but not for 2-aminopropanol. The sign of the calculated optical rotation is correctly predicted by means of PCM, but its magnitude is somewhat underestimated in comparison with experiment for lactamide and overestimated for 2-aminopropanol. To some extent it is rectified by employing explicit hydration. Overall, microsolvation with geometry optimization seems more cost-effective than classical MD, but this is likely to be a consequence of inadequate classical potential and electronic structure model.

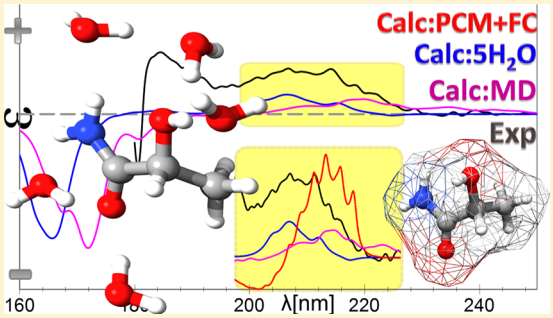

INTRODUCTION

Electronic circular dichroism (CD) and optical rotation (OR), manifestations of natural optical activity, form the basis of the oldest and most widely used methods of chiroptical spectroscopy. Chiroptical spectroscopic methods have been recognized early on as sensitive probes of molecular structure, and since the first works of Arago and Biot in 1811 and 1812,[1,2] much effort has been devoted to understanding the connection between CD and OR and the structure of a chiral system. However, it turned out that the empirical rules connecting molecular structure with electronic circular dichroism spectra (e.g., the quadrant and octant rules) have a limited range of applications.[3] Finding such correlation was even more difficult in the case of specific optical rotation.[4] In this situation, the use of circular dichroism spectra or optical rotation to establish the absolute configuration was often problematic and could lead to wrong conclusions.[4,5]

This has changed to some extent in recent years, when it has become possible to calculate chiroptical spectra of sizable systems of chemical interest using methods of quantum chemistry.[6−8] Quantum chemical modeling provided an opportunity to establish the unknown absolute configuration of an optically active molecule by comparing a calculated spectrum and an experimental one.[9−12] Another field of research combining CD measurements with ab initio calculations is conformational studies, where chiroptical methods are used to derive information about the conformations of a flexible molecule.[13−18]

In both these fields of application, it is important to account for the fact that chiroptical spectra are extremely sensitive to solvent effects[19−25] and molecular geometry.[23,26−29] This is true for natural optical rotation (OR) (which can even change sign with a change of solvent[30,31]) and also for other chiroptical phenomena, such as electronic circular dichroism,[21,23,27,32] vibrational circular dichroism (VCD),[33−35] and vibrational Raman optical activity (ROA).[36,37] The solvent effect is particularly pronounced for polar molecules in an aqueous environment, where hydrogen bonds are formed. This often complicates the band assignment when interpreting the spectra. Therefore, modeling of the solvent influence on electronic circular dichroism and optical rotatory dispersion spectral parameters is of paramount importance in the calculations of chiroptical spectra.[21,38] It is also essential to account for all conformations of a flexible molecule in a computational study.

There are two main "approaches" used for modeling the influence of a solvent surrounding an optically active molecule on its chiroptical properties:[38] those where only the solute molecule is treated quantum mechanically (QM) and the

Received: January 17, 2013
Revised: March 24, 2013
Published: March 26, 2013

   dx.doi.org/10.1021/jp400562n | J. Phys. Chem. B 2013, 117, 5136−5147

solvent is treated as a source of electrostatic potential, and those where both the solute molecule and the solvent molecules are treated as quantum systems. In the first approach, the solvent is either assumed to be homogeneous and isotropic and is modeled as a macroscopic dielectric continuum medium characterized by a scalar dielectric constant (several varieties of the polarizable continuum models, PCM,[39−45]) or is treated as an assembly of discrete charges (or point dipoles), usually obtained from molecular dynamics simulations. Molecular dynamics (classical or quantum mechanical) can also be used in the second approach, where both the solute molecule and some neighboring molecules of the solvent are explicitly included in the quantum chemical calculations at the same or different level of theory (the supermolecular approach). The first approach (usually involving PCM calculations) is much less expensive in terms of computing time but fails to describe specific interactions such as hydrogen bonds.

In the present article, we are going to compare the performance of two methods of modeling spectra—implicit (PCM) and explicit (microsolvation with the positions of water molecules obtained either from MD simulations or geometry optimization) solvent models for electronic circular dichroism and optical rotation of *R*-(+)-lactamide and *S*-(+)-2-aminopropanol. In the implicit solvent model calculations, also the vibrational structure of the CD spectrum of lactamide has been evaluated. Such comparison has been shown before for Raman optical spectra (ROA) of these molecules,[46] and now we extend it to electronic chiroptical spectra. We also compare the performance of a Coulomb-attenuated DFT functional and a conventional hybrid DFT functional for OR and CD.

This study is structured as follows. First, the experimental and computational details are described. Next, we discuss the collected experimental CD and absorption spectra of lactamide and 2-aminopropanol, and then compare how several methods of modeling the hydration effects (polarizable continuum model, molecular dynamics, and microsolvation by a small number of water molecules) reproduce them. We pay particular attention to the role of first and second solvation shells and to the influence of the number of snapshots taken into account in the simulations on the obtained spectrum. An analogous analysis is repeated for the optical rotation and its dispersion. Finally, the main conclusions and a summary are presented.

COMPUTATIONAL AND EXPERIMENTAL DETAILS

Computational Details. The influence of the aqueous environment on the structures of *R*-(+)-lactamide and *S*-(+)-2-aminopropanol has been modeled in three different ways: by means of PCM calculations, molecular dynamics simulations, and using a microsolvation model with explicit water molecules.

The structures used for the continuum model calculations have been optimized using the conductor-like polarized continuum model (C-PCM)[42−44] with the B3LYP[47,48] and CAM-B3LYP[49] functionals and the aug-cc-pVTZ[50] basis set. Both geometry optimization and all calculations of optical properties have been carried out using the Gaussian 09[51] program package. When B3LYP is employed, lactamide has four stationary conformers with Boltzmann weights at room temperature of 46.9%, 22.1%, 17.4%, and 13.6%, respectively (as obtained using the Gaussian 09 implementation of C-PCM, which differs from the one in Gaussian 03 used for our previous calculations of the ROA spectra),[46] while 2-aminopropanol has six conformers. Contribution of the lowest-lying one is 93.2%, contributions of the others are around 1% each. The lowest-lying conformers of both molecules are shown in Figure 1. The optimization with Gaussian 09 with C-PCM and the CAM-B3LYP functional also yields 4 stable conformers for lactamide, but with different Boltzmann weights: 72.6%, 10.5%, 9.7% and 7.2%. For 2-aminopropanol the Boltzmann weight of the lowest-energy conformer increases to 94.4% when CAM-B3LYP is used instead of B3LYP, while other contributions are around 1% each.

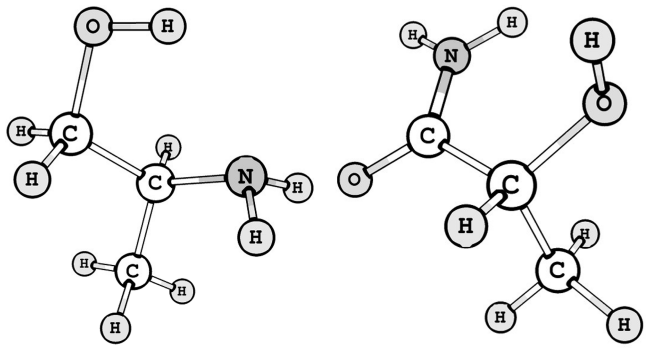

Figure 1. Structures of the lowest-energy conformers of *S*-(+)-2-aminopropanol (left) and *R*-(+)-lactamide (right).

The implicit modeling of solvent effects on the chiroptical properties also has been carried out using the polarized continuum model with two different approaches: conductor-like PCM (C-PCM) and integral equation formalism PCM (IEF-PCM).[40,41] The results from the two different PCM approaches are almost the same for the CD spectra; therefore, only the results from the C-PCM approach are described in the present article. CD spectra and OR for both molecules have been calculated using the aug-cc-pVTZ basis set and two functionals: B3LYP[47,48] and CAM-B3LYP.[49]

Calculations of the vibrational structure of the ECD spectra[52,53] have been performed with a locally modified version of the Gaussian program[51] employing the vertical gradient (VG) approach (also referred to as linear coupling model (LCM)[54]). This model (see ref 55 and references therein for more details) is based on the assumption that the harmonic potential energy surface (PES) in the excited state retains the same shape as in the ground state, apart from a shift of the equilibrium geometry. The information on the shift along the normal modes between the initial and final states is obtained from the energy gradients in the excited state at the equilibrium geometry of the ground state.

Ground- and excited-state computations have been performed for four conformers at the DFT/time-dependent DFT[56] level, respectively, with the CAM-B3LYP functional and the aug-cc-pVTZ basis set. In a second step, these data have been used to obtain vibrationally resolved ECD spectra. Taking into account the nature of the absorption transition, the energy difference between both electronic states involved in the transition has been replaced by the value computed with the nonequilibrium solvation model within the linear response regime.[57,58] In order to simulate homogeneous broadening of the spectrum lines, vibronic stick-spectra have been convoluted using Lorentzian functions with a half-width at half-maximum (HWHM) of 200 cm^{-1}.

Molecular dynamics (MD) calculations have been performed using the TINKER program.[59] MD trajectories have been run for 1 and 10 ns at constant temperature (298 K) and pressure

dx.doi.org/10.1021/jp400562n | J. Phys. Chem. B 2013, 117, 5136−5147

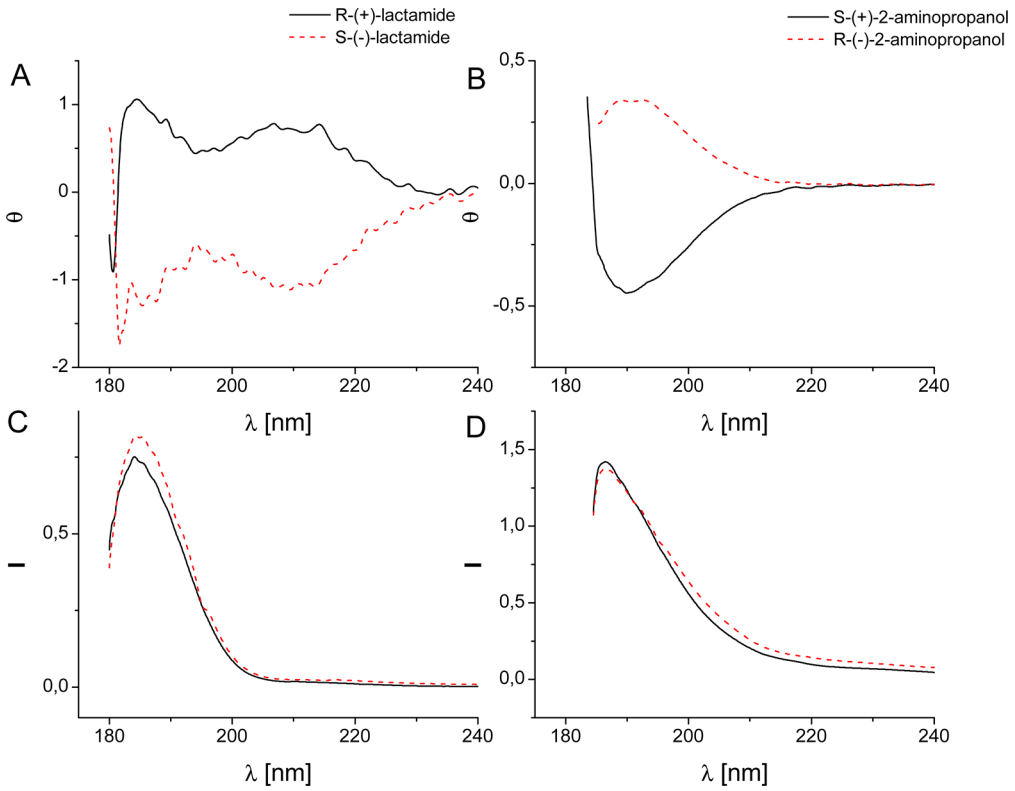

Figure 2. Experimental CD (A, B) and absorption (C, D) spectra of both enantiomers of lactamide (A, C) and 2-aminopropanol (B, D).

(1 atm). Further details can be found in ref 46. The DFT B3LYP and CAM-B3LYP calculations of optical responses have been performed for 400 snapshots from the 10 ns simulation, and the CD spectrum and OR have been calculated as an average. One hundred snapshots from the shorter trajectory for *R*-(+)-lactamide have been used to study the influence of the number of water molecules on the calculated CD spectra and OR. They have been divided into three groups, the criterion being the distance of H_2O molecules from lactamide and the existence of hydrogen bonds between them. The DFT-B3LYP calculations of CD and OR have been carried out for clusters containing water molecules bonded to the molecule under study via hydrogen bonds within a distance of 3.6 Å from lactamide (5−12 water molecules), for the first solvation sphere (all water molecules within the distance of 3.6 Å: 9−16 water molecules per cluster) and for the second solvation sphere (water molecules within the distance of 5 Å from the solute: 23− 35 waters). The remaining solvent has been modeled by means of C-PCM.

The last method used to reproduce the influence of the aqueous environment on lactamide and 2-aminopropanol is the microsolvation model based on QM geometry optimization with explicit water molecules hydrogen-bonded to the solute. Five water molecules have been added to each stable conformer of lactamide and 2-aminopropanol. Optimization of clusters has been performed at the DFT/B3LYP/aug-cc-pVTZ computational level, again using C-PCM to account for the remaining part of the solvent. As a result, five structures for each stable conformer have been obtained and used for the calculations of the optical responses using the aug-cc-pVTZ basis set together with the B3LYP and CAM-B3LYP functionals.

For the calculations of the CD spectra, eight excitations have been taken into account, which correspond to the spectral range of 150−350 nm. Modeling of OR has been carried out at different wavelengths (589, 578, 546, 436, 405, and 365 nm). To model the spectra the Lorentz functions with a 5-nm half-width at half-maximum have been employed.

Experimental Details. Experimental CD spectra have been acquired using a Jasco J-715 CD-UV/vis spectropolarimeter at room temperature. The concentrations of aqueous solutions have been 0.00164 mol/L for both enantiomers of 2-aminopropanol and 0.001207 mol/L for *R*-(+)-lactamide and *S*-(−)-lactamide. The measurement range has been 260−183.5 nm.

Optical rotation at the sodium line of 589 nm has been recorded on a JASCO J-715 spectropolarimeter equipped with a 1-mm path length at room temperature. Concentration of aqueous solution has been 0.5001 mol/L for *R*-(+)-lactamide and 0.8647 mol/L for *S*-(+)-2-aminopropanol. It was verified that the specific optical rotation remains the same when the solutions are diluted.

RESULTS

Circular Dichroism Spectra. *Experimental CD Spectra.* First, we will discuss the experimental electronic absorption and CD spectra of lactamide and 2-aminopropanol and attempt to ascribe the bands to the specific excitations on the basis of the microsolvation calculations, which we consider more reliable than the PCM ones (see below).

The experimental spectra of lactamide (Figure 2A and C) exhibit the first band (positive in the CD spectrum of *R*-(+)-lactamide) with maximum at 206.8 nm and a pronounced vibrational structure. It can be ascribed to a $\pi^* \leftarrow$ n transition from the lone-electron pair of oxygen (from the carbonyl group) to the antibonding π^* orbital which is delocalized between nitrogen, carbon, and oxygen. The second band in the

dx.doi.org/10.1021/jp400562n | *J. Phys. Chem. B* 2013, 117, 5136−5147

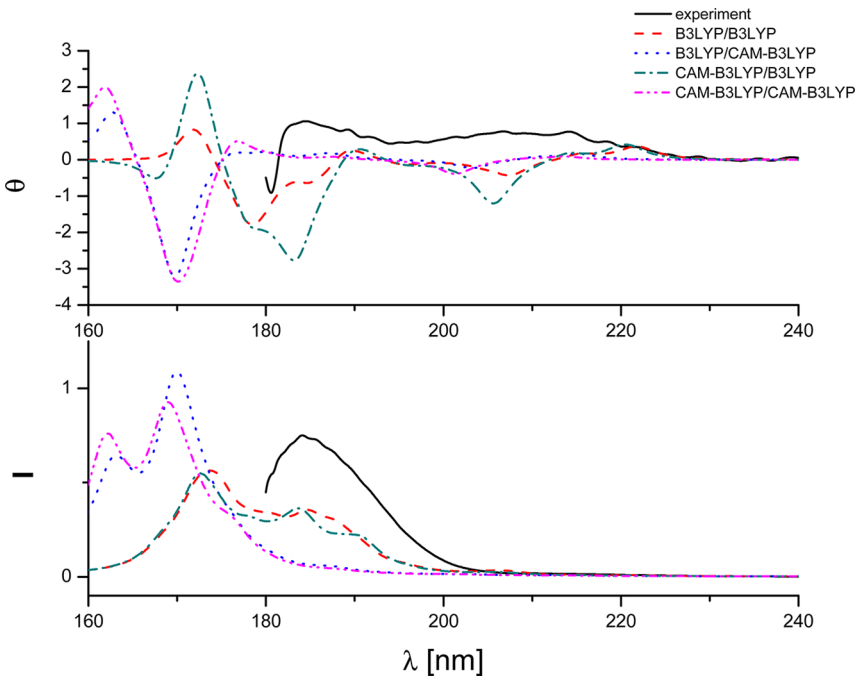

Figure 3. Comparison of the calculated (C-PCM, B3LYP/aug-cc-pVTZ), (C-PCM, CAM-B3LYP/aug-cc-pVTZ), and experimental CD (upper graph) and absorption (lower graph) spectra of *R*-(+)-lactamide. Conformers optimized with the B3LYP and CAM-B3LYP functionals.

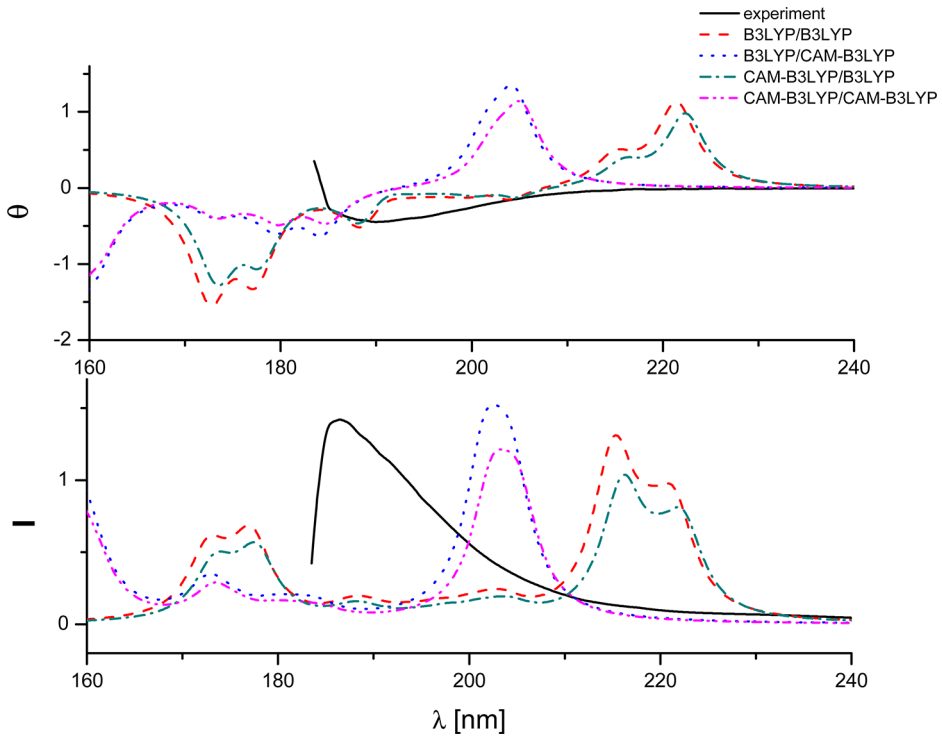

Figure 4. Comparison of the calculated (C-PCM, B3LYP/aug-cc-pVTZ), (C-PCM, CAM-B3LYP/aug-cc-pVTZ) and experimental CD (upper graph) and absorption (lower graph) spectra of *S*-(+)-2-aminopropanol. Conformers optimized with the B3LYP and CAM-B3LYP functionals.

CD spectrum has a maximum at 184.5 nm and appears to correspond to the $\pi^* \leftarrow \pi$ transition to the same orbital. The third excitation occurs at 180.6 nm (a negative CD band for the *R*-(+)-lactamide stereoisomer). It is probably a $\sigma^* \leftarrow \pi$ transition, where σ^* is an antibonding orbital delocalized between carbon atoms and π remains the same as in the second excitation. In the absorption spectrum (Figure 2C) there is only one maximum, at 184.1 nm, the dipole strength of both $\pi^* \leftarrow \pi$ and $\pi^* \leftarrow$ n transitions being close to zero in lactamide. It can be seen in Figure 2A that the experimental CD spectra of both enantiomers are mirror images.

The experimental CD spectrum of *S*-(+)-2-aminopropanol (Figure 2B) shows only one band, with maximum at 189.9 nm. This is the HOMO−LUMO transition of the $\sigma^* \leftarrow$ n nature, from the free electron pair orbital of nitrogen to the antibonding σ orbital delocalized between carbon atoms. The

dx.doi.org/10.1021/jp400562n | *J. Phys. Chem. B* 2013, 117, 5136−5147

maximum of this band in the absorption spectrum (Figure 2D) is placed at 186.5 nm so that it is slightly shifted with respect to CD, which is probably an artifact resulting from the significant bandwidth. Also in the case of 2-aminopropanol the spectra of both enantiomers are mirror images.

Polarizable Continuum Model Calculations. The circular dichroism and absorption spectra of *R*-(+)-lactamide calculated using the C-PCM model of the aqueous environment and different exchange-correlation functionals (B3LYP, CAM-B3LYP) are shown in Figure 3. In the following, we will use the notation (functional employed for optimization)/(functional employed to compute properties).

For lactamide, the calculated absorption spectra are not significantly affected by the choice of functional used for geometry optimizations. However, the functional used for CD calculations has a substantial influence on the shape of the spectra, especially in the high-energy region (unfortunately inaccessible by experiment).

The spectra of lactamide calculated with CAM-B3LYP are significantly shifted to far UV in comparison with experiment, whereas those computed with B3LYP appear slightly red-shifted, assuming the experimental absorption band corresponds to the 183 nm transition in the CAM-B3LYP/B3LYP spectrum, an assumption supported by the comparison of the CD spectra. On the other hand, the profile of the experimental CD spectrum seems to be better reproduced when the CAM-B3LYP functional is used.

The same set of calculations has been carried out for *S*-(+)-2-aminopropanol. The results are displayed in Figure 4. Since the experimental absorption and CD spectra of 2-aminopropanol contain only one band (the molecule absorbs mainly in far UV, which is inaccessible to the spectrometer at our disposal), no definite conclusions concerning the performance of individual functionals in comparison with experiment can be drawn. The excitation energies seem to be underestimated in comparison with experiment for both B3LYP and CAM-B3LYP (more so for the latter). The calculated spectrum depends strongly on the choice of a functional. Not only is the CAM-B3LYP spectrum strongly shifted to far UV, but the number of bands is different than when B3LYP is used. Stronger influence of the range-separation in the functional on the calculated CD spectrum in 2-aminopropanol than in lactamide is probably connected to a different character of electronic transitions in the latter (this might be ascribed to the presence of low-lying Rydberg states for 2-aminopropanol, which are difficult to describe by means of time-dependent DFT with the functionals employed).

The use of CAM-B3LYP instead of B3LYP in geometry optimization (and calculation of Boltzmann weights) does not significantly change the appearance of the calculated absorption and CD spectra of 2-aminopropanol, since the spectra are dominated by a contribution from one conformer, independently of the functional employed.

Vibrational Structure. The first CD band of lactamide exhibits a well visible vibrational structure, and thus, we decided to model it by means of the vertical gradient approximation. The results, as obtained using PCM, are shown in Figure 5. In spite of the relatively simplified model employed for the simulation, the experimental vibrational structure is well reproduced. There is one-to-one correspondence between experimental and calculated vibrational bands, and if the simulated spectrum is red-shifted by 7 nm, their positions and intensities match. These results show that for electronic

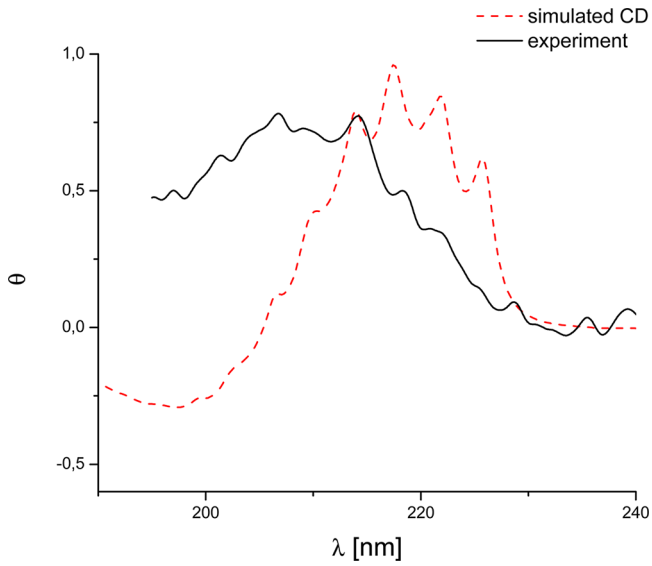

Figure 5. Comparison of the simulated and experimental vibrational structure of the first band of the CD spectrum of *R*-(+)-lactamide.

transitions where no sign changes in ECD spectra are observed, the vibrationally resolved line-shape can be effectively computed with VG models at the Franck−Condon level of approximation. It can be noted that the simulation of vibrational envelopes of ECD spectra can be particularly important for complex CD spectra, which involve delicate cancellations of positive and negative CD bands, as demonstrated by Neugebauer et al. in their gradient-based vertical Franck−Condon simulation of the ECD spectrum of dimethyloxirane.[60] The experimental CD spectrum of 2-aminopropanol (see Figure 2B) does not exhibit a vibrational structure, and vibrational bands were therefore not modeled for this molecule.

Molecular Dynamics. The CD and absorption spectra of *R*-(+)-lactamide and *S*-(+)-2-aminopropanol as calculated using molecular dynamics (MD) snapshots are shown in Figure 6. The region below 180 nm has large contributions from the transitions in water (spurious charge-transfer excitations, as discussed in refs 24,61), but this does not affect the comparison with the experimental spectra, collected in the lower-energy region. The calculated B3LYP absorption spectrum is apparently very close to the experimental one, the only difference being a slight red shift of the calculated spectrum vs experiment (189.6 nm vs 184.6 nm, respectively). This is, however, not the case with the CD spectrum, which would approximately correspond to experiment if the red shift was much larger. Employing the CAM-B3LYP functional to compute CD and absorption spectra of *R*-(+)-lactamide from 400 MD-generated structures produces the spectra shifted to far UV with respect to the experimental data by approximately 10 nm. The first and second excitation bands have lower rotatory strengths than in the case of the B3LYP spectra. In comparison with the experimental spectra of *R*-(+)-lactamide, B3LYP appears to perform somewhat better than CAM-B3LYP. Because of the limited comparison with the experiment and the computational cost involved in calculations for 400 structures, we decided not to repeat the calculations for 2-aminopropanol with the CAM-B3LYP functional.

Similarly to that of lactamide, the MD simulation in combination with B3LYP renders the absorption spectrum of

dx.doi.org/10.1021/jp400562n | *J. Phys. Chem. B* 2013, 117, 5136−5147

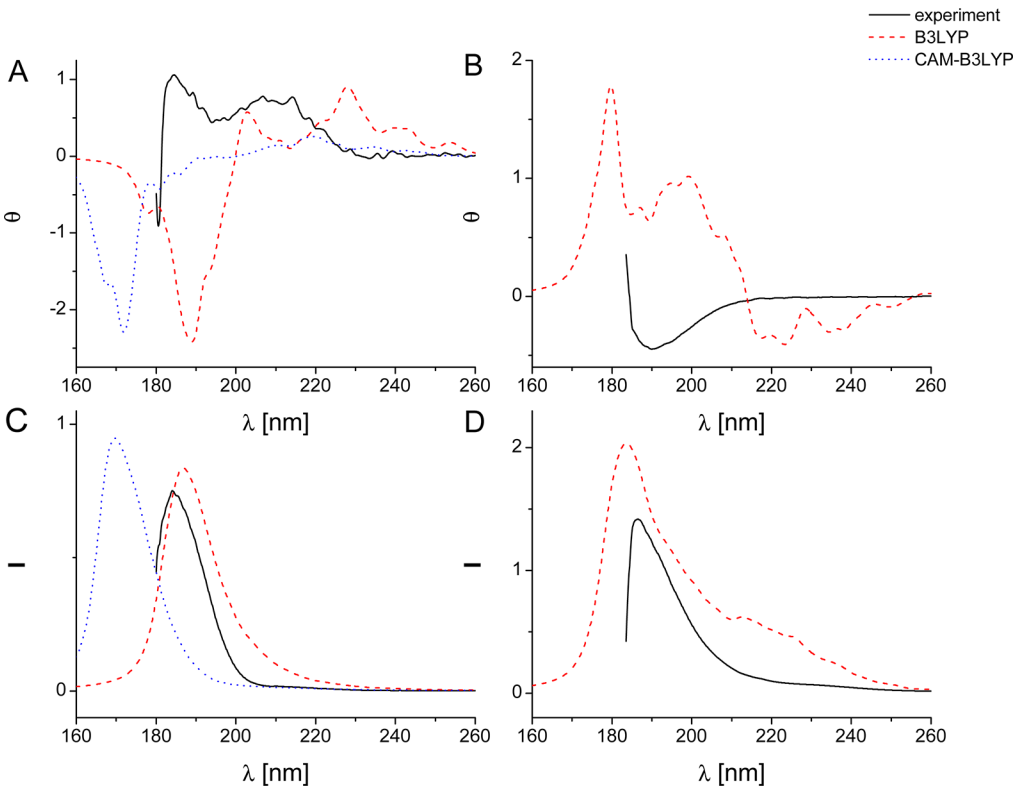

Figure 6. Comparison of the calculated (400 MD snapshots, B3LYP/aug-cc-pVTZ and CAM-B3LYP/aug-cc-pVTZ) and experimental CD (A, B) and absorption (C, D) spectra of *R*-(+)-lactamide (A, C) and *S*-(+)-2-aminopropanol (B, D).

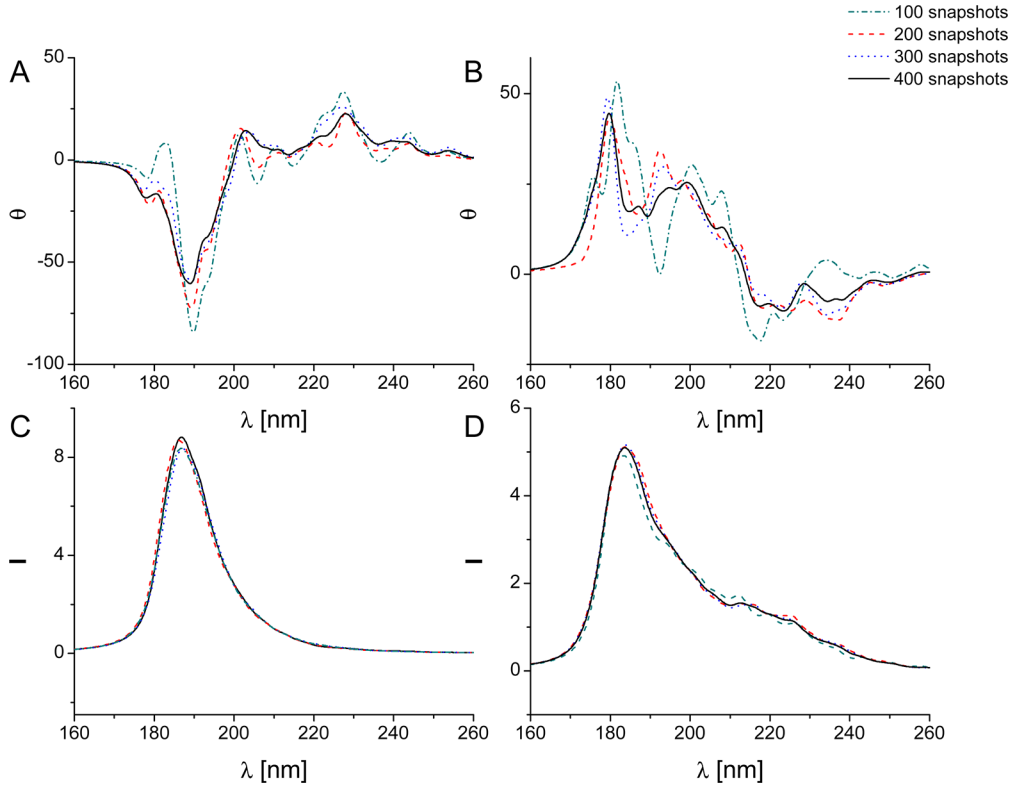

Figure 7. Comparison of the CD (A, B) and absorption (C, D) spectra of *R*-(+)-lactamide (A, C) and *S*-(+)-2-aminopropanol (B, D) calculated from 100, 200, 300, and 400 MD snapshots. B3LYP/aug-cc-pVTZ.

2-aminopropanol close to the experiment (excitations at 267, 250, 235, 221, 199, 188, and 180 nm, the intensity of the last one being the highest), but the calculated CD spectrum is very unlike the experimental one (Figure 6B).

dx.doi.org/10.1021/jp400562n | *J. Phys. Chem. B* 2013, 117, 5136−5147

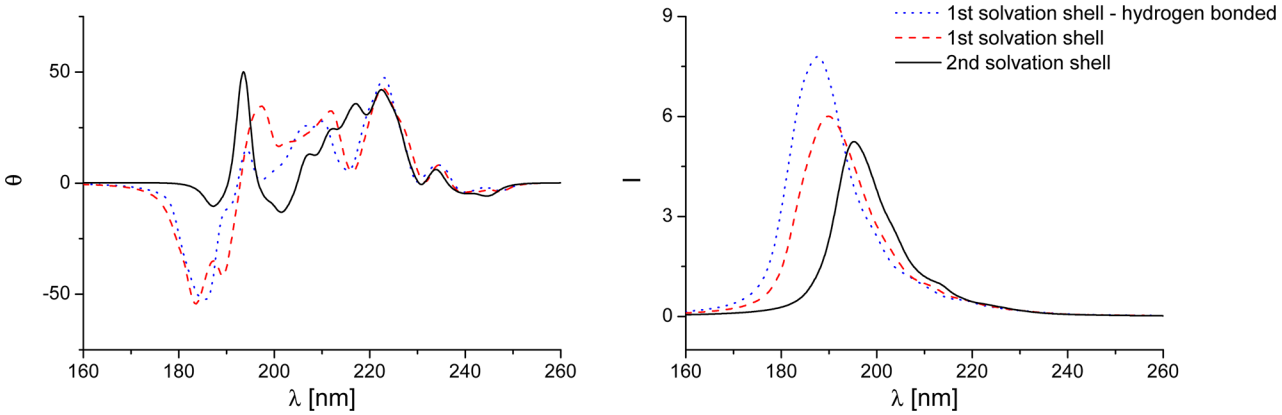

Figure 8. Comparison of the CD (left graph) and absorption (right graph) spectra of *R*-(+)-lactamide calculated including the first hydrogen-bonded solvation shell, the complete first solvation shell, and the second solvation shell.

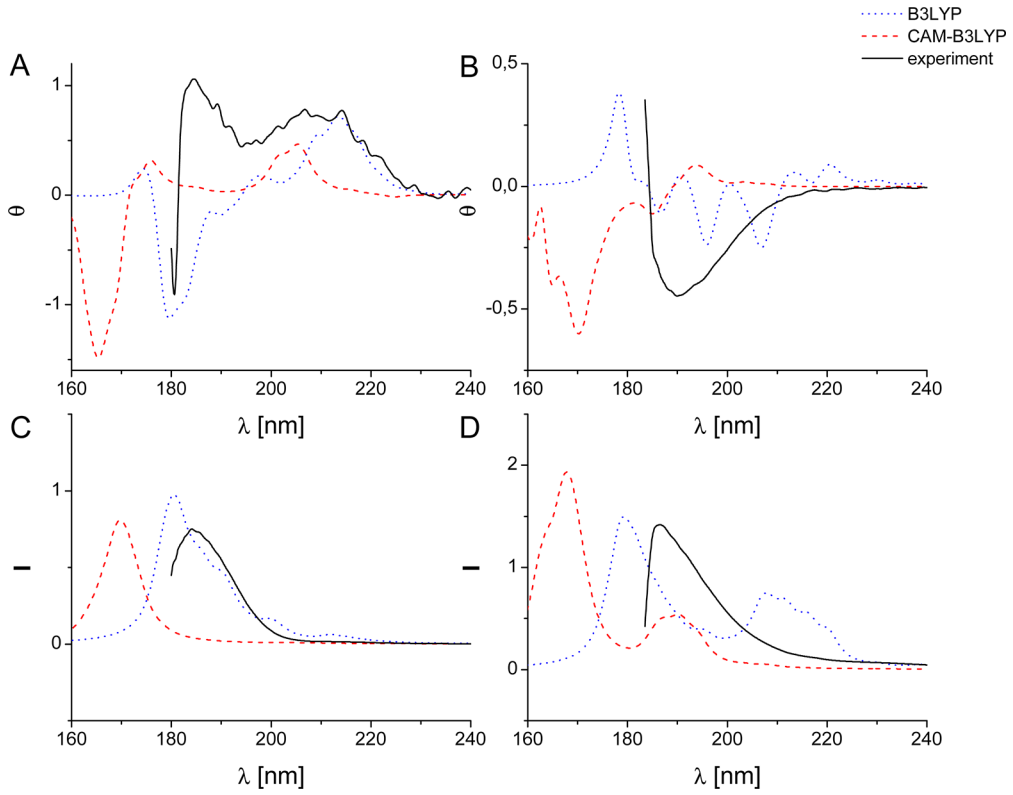

Figure 9. Comparison of the CD (A, B) and absorption (C, D) spectra of *R*-(+)-lactamide (A, C) and *S*-(+)-2-aminopropanol (B, D) calculated using the microsolvation model with five water molecules at the (C-PCM, CAM-B3LYP/aug-cc-pVTZ), (C-PCM, B3LYP/aug-cc-pVTZ) levels of theory with experiment.

The dependence of the calculated spectra of *R*-(+)-lactamide and *S*-(+)-2-aminopropanol on the number of MD snapshots averaged in the simulations has been investigated by comparing the spectra collected using 100, 200, 300, and 400 MD-generated structures. Figure 7 shows how increasing the number of MD geometries changes the appearance of the simulated CD and absorption spectra. For lactamide, most of the excitations have the same wavelength independently of the number of snapshots, and the sign of the CD bands generally remains the same, but the intensity of the peaks changes significantly. Some bands (for example that at 208 nm) which are visible in the spectrum simulated from 100 MD structures disappear for a larger number of structures. Similar observations can be made from the analogous study for 2-aminopropanol: when comparing the spectra from 100 and 300 MD geometries, it can be seen that some of the bands disappear with the increasing number of snapshots (e.g., the band at 176 nm) and that some of the smaller bands change signs (e.g., 237 nm). For both molecules the differences between the spectra collected from 200 and 400 MD geometries are small, and thus it seems that 200−300 MD geometries are sufficient for the simulations of the CD spectra. The simulated absorption spectra have maxima at the same wavelengths for all simulations (100, 200, 300, and 400 MD structures), and even 100 snapshots seem enough to reliably model the absorption spectra as far as the intensity is concerned. Vibrational Raman and Raman optical activity spectra are more demanding in this respect.[46]

dx.doi.org/10.1021/jp400562n | *J. Phys. Chem. B* 2013, 117, 5136−5147

Table 1. Optical Rotation for *R*-(+)-Lactamide and *S*-(+)-2-Aminopropanol Calculated by Means of C-PCM and IEF-PCM with the aug-cc-pVTZ Basis Set[a]

	α [deg dm^2 mol^{-1}]							
	R-(+)-lactamide				*S*-(+)-2-aminopropanol			
γ [nm]	C-PCM B3LYP	C-PCM CAM-B3LYP	IEF-PCM B3LYP	IEF-PCM CAM-B3LYP	C-PCM B3LYP	C-PCM CAM-B3LYP	IEF-PCM B3LYP	IEF-PCM CAM-B3LYP
589	5.01	5.68	4.67	4.63	12.03	12.10	11.93	10.95
578	5.21	5.89	4.86	4.82	12.53	12.60	12.43	11.40
546	5.90	6.59	5.48	5.43	14.20	14.27	14.08	12.90
436	9.73	10.17	8.98	8.82	23.64	23.74	23.46	21.26
405	11.59	11.65	10.66	10.39	28.17	28.29	27.98	25.20
365	15.10	13.97	13.79	13.19	36.50	36.61	36.27	32.28

[a]The structures have been optimized with the B3LYP functional.

Another question which emerges in the simulations of the solvation effects from MD-generated structures (or, indeed, in all supermolecular simulations of solvent effects) is how many solvent molecules should be accounted for in the simulations to reproduce the main features of the solvent effect. We have therefore analyzed how the number of water molecules in MD clusters affects the shape of the CD spectrum of lactamide. For this purpose, we have compared the spectra calculated for clusters containing only (i) water molecule forming direct hydrogen bonds with lactamide, (ii) all water molecules of the first solvation shell, and (iii) all water molecules of the second solvation shell (classification criteria have been described in the Computational Details section). The results are shown in Figure 8. The number of water molecules in MD clusters turned out to affect the spectra significantly, especially the addition of a second solvation shell. When comparing the spectra calculated for the hydrogen-bonded first solvation shell and the whole first solvation shell, one can observe that the band at 189 nm changes sign. Further addition of water molecules (second solvation shell) changes the sign of the 182 and 194 nm bands. This is understandable, considering that in the region below 195 nm there are strong contributions from excitations in water molecules, coupled with transitions in lactamide. The intensity of low-energy peaks (with no contributions from transitions in water) is modified, too (although to a lesser extent), so that the shape of the spectrum changes substantially, even though the excitation energies are usually unaffected by the number of water molecules.

Microsolvation Model. Now, we shall proceed to the discussion of the performance of the microsolvation model (surrounding the molecule in question by a small number of solvent molecules and carrying out geometry optimization for several such structures) for simulations of the electronic spectra of lactamide and 2-aminopropanol. The absorption and CD spectra of *R*-(+)-lactamide and *S*-(+)-2-aminopropanol calculated for the optimized clusters containing the solute molecule interacting with five water molecules are shown in Figure 9.

The CD spectrum of *R*-(+)-lactamide (Figure 9A) calculated using B3LYP bears little resemblance to the experimental one, even though the excitation energies seem to be correctly predicted: the sign of the lowest-energy band is in agreement with experiment, but the sign of the next band is not. CAM-B3LYP is more successful in predicting the CD intensities (all the signs are rendered correctly, although the relative intensity of the 176 nm band is underestimated in comparison with that of experiment); thus, we consider this simulation relatively reliable, and we have used it to ascribe the signals to the individual transitions (see subsection Experimental CD Spectra), even though the blue shift in comparison with experiment is much larger for CAM-B3LYP than for B3LYP.

In the calculated CD spectrum of *S*-(+)-2-aminopropanol (Figure 9B) the sign of the lowest-energy band is reproduced correctly, independently of the functional employed. The very small number of bands in the CD and absorption spectrum precludes a more detailed discussion. Similarly to PCM calculations, not only are B3LYP and CAM-B3LYP spectra shifted with respect to each other, but the intensities are completely different.

Optical Rotation. Now, the performance of different solvent models in the calculations of optical rotation and optical rotatory dispersion will be discussed. The calculations of optical rotation have been carried out by means of the same method as used to compute the CD spectra. The experimental optical rotation of *R*-(+)-lactamide for sodium 589 nm line is 7.25 deg·dm^2·mol^{-1}, and of *S*-(+)-2-aminopropanol 4.20 deg·dm^2·mol^{-1}. The values are small so that reproducing them by means of computational methods without large relative errors is challenging.

Polarizable Continuum Model. The optical rotation calculated for *R*-(+)-lactamide and *S*-(+)-2-aminopropanol using the polarizable continuum model is displayed in Table 1. The obtained values have the correct signs for both molecules, independently of the functional and continuum model variation employed, and their magnitudes for lactamide are in a very good agreement with the experiment. Using the CAM-B3LYP functional instead of B3LYP with the C-PCM approach increases very slightly the calculated optical rotation for both molecules, taking it farther away from experiment in the case of *S*-(+)-2-aminopropanol, but bringing it closer for *R*-(+)-lactamide. CAM-B3LYP thus does not provide a consistent improvement of the calculated optical rotation over B3LYP, and this observation is in agreement with previous works on this subject.[62,63]

The CAM-B3LYP results are more sensitive to the employed solvent model (C-PCM vs IEF-PCM) than the B3LYP ones, but overall these two different ways of modeling interaction with polarizable continuum model lead to very similar results. The same has been observed for the CD spectra of these molecules and for the ROA spectra.[46] Thus, the two approaches are practically interchangeable for calculations of chiroptical spectra.

We have also calculated the dependence of the optical rotation on the incident light wavelength (optical rotatory dispersion, ORD), calculating the optical rotation for the wavelengths of 589, 578, 546, 436, 405, and 365 nm. Optical rotation of both molecules increases in the absolute value with

dx.doi.org/10.1021/jp400562n | J. Phys. Chem. B 2013, 117, 5136−5147

the energy of incident light, as usual in the below-resonance region.[64,65] The calculated slope is lower if the CAM-B3LYP functional is used instead of B3LYP, probably because the calculated poles (corresponding to electron excitations) shift to higher-energy values when the Coulomb-attenuated functional is used.

Employing CAM-B3LYP instead of B3LYP for geometry optimization leaves the OR values practically unchanged, and thus, this issue will not be discussed any further.

Molecular Dynamics. The optical rotations of *R*-(+)-lactamide and *S*-(+)-2-aminopropanol with explicitly bonded water molecules have been calculated using MD snapshots. The resulting values, shown in Table 2, calculated for clusters with

Table 2. Optical rotation for *R*-(+)-Lactamide and *S*-(+)-2-Aminopropanol Calculated from 300 MD Snapshots with the aug-cc-pVTZ Basis Set and B3LYP Functional

	α [deg dm^2 mol^{-1}]	
λ [nm]	*R*-(+)-lactamide	*S*-(+)-2-aminopropanol
589	20.47	13.23
578	21.38	13.76
546	24.43	15.49
436	42.76	24.71
405	52.27	28.75
365	71.09	35.33

the first and second solvation shell (on the average containing different numbers of water molecules, see Computational Details) are significantly overestimated. In our opinion, this is a consequence of a fundamental problem with the calculations of optical rotation for supermolecular clusters: optical rotation (like molecular polarizability) is an extensive property. Therefore, although in the case of a solvated molecule the induced chirality of the ordered solvent most probably contributes to the total optical rotation, calculations for a large solute−solvent cluster are likely to lead to artificially large values. Spurious charge-transfer excitations may also be a factor influencing optical rotation for these systems.[24,61]

The issue has been investigated further and we have carried out the calculations for lactamide−water clusters containing from 5 to 12 water molecules. From 3 to 82 MD-generated structures have been taken into account for each number of water molecules, and the results have been averaged out. The results, gathered in Table 3, show that a larger number of water molecules, as a rule, leads to a larger OR value, but the increase with the number of water molecules is not monotonic, probably as a consequence of different numbers of clusters taken into account for each number of water molecules. All the results are significantly overestimated in comparison with the experimental OR value for *R*-(+)-lactamide.

Microsolvation. The optical rotation calculated for *R*-(+)-lactamide and *S*-(+)-2-aminopropanol surrounded by five water molecules is shown in Table 4: addition of water

Table 4. Optical Rotation for *R*-(+)-Lactamide and *S*-(+)-2-Aminopropanol Calculated with the Microsolvation Approach with the aug-cc-pVTZ Basis Set[a]

	α [deg dm^2 mol^{-1}]			
	R-(+)-lactamide		*S*-(+)-2-aminopropanol	
λ [nm]	B3LYP	CAM-B3LYP	B3LYP	CAM-B3LYP
589	2.02	1.73	2.91	−0.06
578	2.13	1.82	3.03	−0.06
546	2.54	2.15	3.41	−0.07
436	5.46	4.46	5.49	−0.11
405	7.28	5.84	6.41	−0.13
365	11.39	8.85	7.92	−0.17

[a]Structures have been optimized with the B3LYP functional.

molecules decreases the optical rotation of both systems. In the case of CAM-B3LYP calculations for *S*-(+)-2-aminopropanol even the sign changes. For both molecules, the microsolvation results are somewhat underestimated in comparison with experiment. It is expected that further addition of water molecules would increase again the calculated OR for both molecules (as in the case of MD snapshots, see above), bringing it into better agreement with experiment.

We have also calculated ORD for both molecules surrounded by five water molecules. The slope of OR dispersion for both molecules under study is smaller when water molecules are explicitly included than for the PCM-only calculations. This is probably related to a slight shift of the excitation energies to farther UV when explicit water molecules are included.

SUMMARY AND CONCLUSIONS

Electronic circular dichroism spectra and optical rotation have been measured and calculated using time-dependent density functional theory for aqueous solutions of lactamide and 2-aminopropanol. The choice of the molecules has been motivated by the previous study of the vibrational Raman optical activity spectra in these systems. The solvent models employed in this study are the polarizable continuum model (Conductor-like PCM (C-PCM) and Integral Equation Formalism PCM (IEF-PCM) varieties) and explicit solvation coupled with PCM, with solute−solvent clusters generated either by molecular dynamics or geometry optimization. The vibrational structure of the band corresponding to the HOMO−LUMO transition in lactamide has been calculated. The most important conclusions can be summarized as follows.

Table 3. Optical Rotation for *R*-(+)-Lactamide As a Function of the Number of Water Molecules in MD Cluster

λ [nm]	α [deg dm^2 mol^{-1}]							
number of water molecules	5	6	7	8	9	10	11	12
589	14.4	40.7	19.2	14.8	24.5	16.7	19.9	54.1
578			20.0	15.5	25.6	17.4	20.8	
546			22.6	17.8	29.2	19.9	23.9	
436			37.4	32.4	51.0	35.0	42.7	
405			44.4	40.3	62.3	42.9	52.6	
365	49.5	133.0	57.2	56.9	84.9	58.1	72.7	198.3

dx.doi.org/10.1021/jp400562n | J. Phys. Chem. B 2013, 117, 5136−5147

The signs of the bands in the CD spectrum of lactamide (although not necessarily their relative intensities) are correctly reproduced using all three methods under investigation, at least when the CAM-B3LYP functional is used. This is not the case for 2-aminopropanol, where most simulations are apparently not successful. The calculated spectrum which bears the most resemblance to the experiment is the one obtained using the microsolvation model (with the B3LYP functional), but this may be coincidental because of the small scope for comparison in this case (only one band has been registered in the experimentally available spectral region). The sign of the optical rotation calculated using PCM is correctly predicted, but its magnitude is somewhat underestimated in comparison with experiment for lactamide and overestimated for 2-aminopropanol. Addition of five water molecules decreases the calculated optical rotation for both systems, while further hydration increases it. It should be taken into account that both optical rotations are small in their absolute values, and considering the large errors associated with DFT calculations of optical rotation, the agreement of the sign with experiment may be coincidental.

For the PCM calculations, we can see that the choice of the functional for the geometry optimization does not affect strongly the calculated spectra. Two different ways of modeling the polarizable continuum, C-PCM and IEF-PCM, lead to similar results for both CD spectra and optical rotation.

The functional used for CD calculations has a substantial influence on the shape of the spectra in all solvent models, especially in the high-energy region (unfortunately inaccessible by experiment). The position of the bands seems to be better described when using B3LYP (employing the CAM-B3LYP functional causes a large blue shift of the spectra), but the shape is usually better rendered by means of CAM-B3LYP.

The vertical gradient model employed for the simulation of vibrational structure reproduces well the line-shape of the experimental CD spectrum of lactamide.

Important factors in MD simulations of solvated molecules are the number of snapshots and the number of solvent molecules taken into account. For both molecules, the differences between the spectra collected from 200 and 400 snapshots are small; thus, it seems 200−300 snapshots are sufficient for the simulations of CD spectra (in contrast to the simulations of the ROA spectra[46]). While the number of snapshots does not change the shape of the spectra significantly, the number of water molecules in the MD clusters does, especially the inclusion of the second solvation shell. Overall, no consistent improvement of the results over the microsolvation method or even PCM is observed when MD is used, which may result both from inadequacy of the employed force field (designed primarily for biopolymers) and of the exchange correlation functional.

AUTHOR INFORMATION

Corresponding Author

*E-mail: mpecul@chem.uw.edu.pl.

Notes

The authors declare no competing financial interest.

ACKNOWLEDGMENTS

We thank Dr. Malgorzata Biczysko for many helpful discussions and Professor Jadwiga Frelek for the CD spectra measurements. This work has received support from the Wrocław Centre for Networking and Supercomputing, the high performance computer facilities of the DREAMS center (http://dreamshpc.sns.it) and the Norwegian Supercomputing Program (Notur) through grants of computer time. The project has been carried out with the use of CePT infrastructure financed by the European Union - the European Regional Development Fund within the Operational Programme "Innovative economy" for 2007−2013. The support of COST-CMTS Action CM1002 COnvergent Distributed Environment for Computational Spectroscopy (CODECS) STSM Grants for M.P and A.P and the Polish National Science Center Grant 2012/05/B/ST4/01236 are also acknowledged. A.P. was supported by the Research Council of Norway via an Yggdrasil Grant (210973/F11). K.H.H. was supported by the Norwegian Research Council through a Center of Excellence Grant (179568/V30).

REFERENCES

(1) Arago, D. F. J. Mémoire sur une modification remarquable qu'éprouvent les rayons lumineux dans leur passage à travers certains corps diaphanes et sur quelques autres phénomènes d'optique (Memory on a remarkable change experienced by light rays in their passage through certain transparent bodies and some other optical phenomena. [Engl. Transl.]). *Mém. de l'Inst.* **1811**, *12*, 93−134.

(2) Biot, J. B. Observations sur la nature des forces qui partagent les rayons lumineux dans les cristaux doués de la double réfraction. (Comments on the nature of the forces that share the light rays in the crystal endowed with double refraction. [Engl. Transl.]). *Mém. l'Inst.* **1814**, *14*, 221−234.

(3) Djerassi, C. *Optical Rotatory Dispersion: Applications to Organic Chemistry*; McGraw-Hill Book Company, Inc.: New York, 1960.

(4) Polavarapu, P. L.; Petrovic, A.; Wang, F. Intrinsic Rotation and Molecular Structure. *Chirality* **2003**, *15*, S143−S149.

(5) Polavarapu, P. L. Optical Rotation: Recent Advances in Determining the Absolute Configuration. *Chirality* **2002**, *14*, 768−781.

(6) Pecul, M.; Ruud, K. The Ab Initio Calculation of Optical Rotation and Electronic Circular Dichroism. *Adv. Quantum Chem.* **2005**, *50*, 185−212.

(7) Autschbach, J. Computing Chiroptical Properties with First-Principles Theoretical Methods: Background and Illustrative Examples. *Chirality* **2009**, *21*, E116−E152.

(8) Lauceri, R.; D'Urso, A.; Mammana, A.; Purrello, R. Transfer of Chirality for Memory and Separation. *Top. Curr. Chem.* **2011**, *298*, 143−188.

(9) McCann, D. M.; Stephens, P. J. Determination of Absolute Configuration Using Density Functional Theory Calculations of Optical Rotation and Electronic Circular Dichroism: Chiral Alkenes. *J. Org. Chem.* **2006**, *71*, 6074−6098.

(10) Wang, Y.; Raabe, G.; Repges, C.; Fleischhauer, J. Time-Dependent Density Functional Theory Calculations on the Chiroptical Properties of Rubroflavin: Determination of its Absolute Configuration by Comparison of Measured and Calculated CD Spectra. *Int. J. Quantum Chem.* **2003**, *93*, 265−270.

(11) Braun, M.; Hohmann, A.; Rahematpura, J.; Bühne, C.; Grimme, S. Synthesis and Determination of the Absolute Configuration of Fugomycin and Desoxyfugomycin: CD Spectroscopy and Fungicidal Activity of Butenolides. *Chem.—Eur. J.* **2004**, *10*, 4584−4593.

(12) Schühly, W.; Crockett, S. L.; Fabian, W. M. F.; Hyperolactone, C. Determination of its Absolute Configuration by Comparison of Experimental and Calculated CD Spectra. *Chirality* **2005**, *17*, 250−256.

(13) Schippers, P. H.; Dekkers, H. P. J. M. Optical Activity of *β,γ*-Enones: A Quantitative Chirality Rule. *J. Am. Chem. Soc.* **1983**, *105*, 79−84.

(14) Kotovych, G.; Cann, J. R.; Stewart, J. M.; Yamamoto, H.; NMR; Conformational, C. D. Studies of Bradykinin and its Agonists and

Antagonists: Application to Receptor Binding. *Biochem. Cell. Biol.* **1998**, *76*, 257−266.
(15) Zimmer, C.; Birch-Hirschfeld, E.; Weiss, R. CD Studies on the Conformation of Some Deoxyoligonucleotides Containing Adenine and Thymine Residues. *Nucleic Acids Res.* **1974**, *1*, 1017−1030.
(16) Berova, N.; di Bari, L.; Pescitelli, G. Application of Electronic Circular Dichroism in Configurational and Conformational Analysis of Organic Compounds. *Chem. Soc. Rev.* **2007**, *36*, 914−931.
(17) Corrêa, D. H. A.; Ramos, C. H. I. The Use of Circular Dichroism Spectroscopy to Study Protein Folding, Form and Function. *Afr. J. Biochem. Res.* **2009**, *3*, 164−173.
(18) Barone, V.; Baiardi, A.; Biczysko, M.; Bloino, J.; Cappelli, C.; Lipparini, F. Implementation and Validation of a Multi-Purpose Virtual Spectrometer for Large Systems in Complex Environments. *Phys. Chem. Chem. Phys.* **2012**, *14*, 12404−12422.
(19) Müller, T.; Wiberg, K. B.; Vaccaro, P. H. Cavity Ring-Down Polarimetry (CRDP): A New Scheme for Probing Circular Birefringence and Circular Dichroism in the Gas Phase. *J. Phys. Chem. A* **2000**, *104*, 5959−5968.
(20) Kumata, Y.; Furukawa, J.; Fueno, T. The Effect of Solvents on the Optical Rotation of Propylene Oxide. *Bull. Chem. Soc. Jpn.* **1970**, *43*, 3920−3921.
(21) Pecul, M.; Marchesan, D.; Ruud, K.; Coriani, S. Polarizable Continuum Model Study of Solvent Effects on Electronic Circular Dichroism Parameters. *J. Chem. Phys.* **2005**, *122*, 024106.
(22) Pecul, M.; Lamparska, E.; Cappelli, C.; Frediani, L.; Ruud, K. Solvent Effects on Raman Optical Activity Spectra Calculated Using the Polarizable Continuum Model. *J. Phys. Chem. A* **2006**, *110*, 2807−2815.
(23) Crawford, T. D.; Tam, M. C.; Abrams, M. L. The Current State of Ab Initio Calculations of Optical Rotation and Electronic Circular Dichroism Spectra. *J. Phys. Chem. A* **2007**, *111*, 12057−12068.
(24) Kundrat, M. D.; Autschbach, J. Ab Initio and Density Functional Theory Modeling of the Chiroptical Response of Glycine and Alanine in Solution Using Explicit Solvation and Molecular Dynamics. *J. Chem. Theory Comput.* **2008**, *4*, 1902−1914.
(25) Kundrat, M. D.; Autschbach, J. Modeling of the Chiroptical Response of Chiral Amino Acids in Solution Using Explicit Solvation and Molecular Dynamics. *J. Chem. Theory Comput.* **2009**, *5*, 1051−1060.
(26) Pecul, M.; Ruud, K.; Rizzo, A.; Helgaker, T. Conformational Effects on the Optical Rotation of Alanine and Proline. *J. Phys. Chem. A* **2004**, *108*, 4269−4276.
(27) Autschbach, J.; Ziegler, T.; van Gisbergen, S. J. A.; Baerends, E. J. Chiroptical Properties from Time-Dependent Density Functional Theory. I. Circular Dichroism Spectra of Organic Molecules. *J. Chem. Phys.* **2002**, *116*, 6930−6940.
(28) Wiberg, K. B.; Vaccaro, P. H.; Cheeseman, J. R. Conformational Effects on Optical Rotation. 3-Substituted 1-Butenes. *J. Am. Chem. Soc.* **2003**, *125*, 1888−1896.
(29) Wiberg, K. B.; Wang, Y.-G.; Vaccaro, P. H.; Cheeseman, J. R.; Luderer, M. R. Conformational Effects on Optical Rotation. 2-Substituted Butanes. *J. Phys. Chem. A* **2005**, *109*, 3405−3410.
(30) Müller, T.; Wiberg, K. B.; Vaccaro, P. H. Cavity Ring-Down Polarimetry (CRDP): A New Scheme for Probing Circular Birefringence and Circular Dichroism in the Gas Phase. *J. Phys. Chem. A* **2000**, *104*, 5959−5968.
(31) Kumata, Y.; Furukawa, J.; Fueno, T. The Effect of Solvents on the Optical Rotation of Propylene Oxide. *Bull. Chem. Soc. Jpn.* **1970**, *43*, 3920−3921.
(32) Pulm, F.; Schramm, J.; Lagier, H.; Hormes, J. UV/VUV Circular Dichroism Spectra of Bicyclic Ketones: A Comparison Between Gas Phase and Solvent Spectra. *Enantiomer* **1998**, *3*, 315−322.
(33) Cappelli, C.; Corni, S.; Mennucci, B.; Cammi, R.; Tomasi, J. Vibrational Circular Dichroism within the Polarizable Continuum Model: A Theoretical Evidence of Conformation Effects and Hydrogen Bonding for (*S*)-(−)-3-Butyn-2-ol in CCl_4 Solution. *J. Phys. Chem. A* **2002**, *106*, 12331−12339.
(34) Yang, G.; Xu, Y. Vibrational Circular Dichroism Spectroscopy of Chiral Molecules. *Top. Curr. Chem.* **2011**, *298*, 189−236.
(35) Nicu, V. P.; Baerends, E. J.; Polavarapu, P. L. Understanding Solvent Effects in Vibrational Circular Dichroism Spectra: [1,1′-Binaphthalene]-2,2′-diol in Dichloromethane, Acetonitrile, and Dimethyl Sulfoxide Solvents. *J. Phys. Chem. A* **2012**, *116*, 8366−8373.
(36) Pecul, M.; Rizzo, A.; Leszczynski, J. The Vibrational Raman and Raman Optical Activity Spectra of D-Lactic Acid, D-Lactate, and D-Glyceraldehyde: Ab Initio Calculations. *J. Phys. Chem. A* **2002**, *106*, 11008−11016.
(37) Pecul, M. Modelling of Solvent Effects on Chiroptical Spectra. In *Advances in Chiroptical Methods*; Berova, N., Polavarapu, P., Nakanishi, K., Woody, R. W., Eds.; Wiley: New York, 2011; pp 729−746.
(38) Pecul, M.; Ruud, K. Solvent effects on natural optical activity. In *Continuum Polarized Models*; Mennucci, B., Cammi, R., Eds.; Wiley, Chicester, 2007; pp 206−219.
(39) Tomasi, J.; Mennucci, B.; Cammi, R. Quantum Mechanical Continuum Solvation Models. *Chem. Rev.* **2005**, *105*, 2999−3093.
(40) Cances, E.; Mennucci, B.; Tomasi, J. A New Integral Equation Formalism for the Polarizable Continuum Model: Theoretical Background and Applications to Isotropic and Anisotropic Dielectrics. *J. Chem. Phys.* **1997**, *107*, 3032−3041.
(41) Cances, E.; Mennucci, B. New Applications of Integral Equations Methods for Solvation Continuum Models: Ionic Solutions and Liquid Crystals. *J. Math. Chem.* **1998**, *23*, 309−326.
(42) Klamt, A.; Schüürmann, G. COSMO: A New Approach to Dielectric Screening in Solvents with Explicit Expressions for the Screening Energy and its Gradient. *J. Chem. Soc., Perkin Trans. 2* **1993**, 799−805.
(43) Barone, V.; Cossi, M. Calculation of Molecular Energies and Energy Gradients in Solution by a Conductor Solvent Model. *J. Phys. Chem. A* **1998**, *102*, 1995−2001.
(44) Cossi, M.; Rega, N.; Scalmani, G.; Barone, V. Energies, Structures, and Electronic Properties of Molecules in Solution with the C-PCM Solvation Model. *J. Comput. Chem.* **2002**, *24*, 669−681.
(45) Foresman, J.; Keith, T.; Wiberg, K.; Snoonian, J.; Frisch, M. SCIPCM IPCM Solvent Effects. 5. The Influence of Cavity Shape, Truncation of Electrostatics, and Electron Correlation on Ab Initio Reaction Field Calculations. *J. Phys. Chem.* **1996**, *100*, 16098−16104.
(46) Hopmann, K. H.; Ruud, K.; Pecul, M.; Kudelski, A.; Dračinský, M.; Bouř, P. Explicit versus Implicit Solvent Modeling of Raman Optical Activity Spectra. *J. Phys. Chem. B* **2011**, *115*, 4128−4137.
(47) Becke, A. D. Density-Functional Thermochemistry. III. The Role of Exact Exchange. *J. Chem. Phys.* **1993**, *98*, 5648−5652.
(48) Lee, C.; Yang, W.; Parr, R. G. Development of the Colle−Salvetti Correlation-Energy Formula into a Functional of the Electron Density. *Phys. Rev. B* **1988**, *37*, 785−789.
(49) Yanai, T.; Tew, D.; Handy, N. A New Hybrid Exchange-Correlation Functional Using the Coulomb-Attenuating Method (CAM-B3LYP). *Chem. Phys. Lett.* **2004**, *393*, 51−57.
(50) Dunning, T. H.; Peterson, K. A.; Woon, D. E. Basis Sets: Correlation Consistent Basis Sets. In *Encyclopedia of Computational Chemistry*; Schleyer, P. v. R., Clark, N. L. A. T., Gasteiger, J., Kollman, P. A., Schaefer, H. F.III, Schreiner, P. R., Eds.; Wiley: Chichester, 1998; pp 88−115.
(51) Frisch, M. J.; et al. *Gaussian 09*, Revision A. 02; Gaussian, Inc.: Wallingford, CT, 2009.
(52) Bloino, J.; Biczysko, M.; Santoro, F.; Barone, V. General Approach to Compute Vibrationally Resolved One-Photon Electronic Spectra. *J. Chem. Theory Comput.* **2010**, *6*, 1256−1274.
(53) Bloino, J.; Biczysko, M.; Santoro, F.; Barone, V. Fully Integrated Approach to Compute Vibrationally Resolved Optical Spectra: From Small Molecules to Macrosystems. *J. Chem. Theory Comput.* **2009**, *5*, 540−554.
(54) Macak, P.; Luo, Y.; Ågren, H. Simulations of Vibronic Profiles in Two-Photon Absorption. *Chem. Phys. Lett.* **2000**, *330*, 447−456.
(55) Biczysko, M.; Bloino, J.; Santoro, F.; Barone, V. Time Independent Approaches to Simulate Electronic Spectra Lineshapes:

from Small Molecules to Macrosystems. In *Computational Strategies for Spectroscopy, from Small Molecules to Nano Systems*; Barone, V., Ed.; Wiley: NY, 2011; pp 361−443.
(56) Scalmani, G.; Frisch, M.; Mennucci, B.; Tomasi, J.; Cammi, R.; Barone, V. Geometries and Properties of Excited States in the Gas Phase and in Solution: Theory and Application of a Time-Dependent Density Functional Theory Polarizable Continuum Model. *J. Chem. Phys.* **2006**, *124*, 094107.
(57) Improta, R.; Barone, V.; Scalmani, G.; Frisch, M. A State-Specific Polarizable Continuum Model Time Dependent Density Functional Theory Method for Excited State Calculations in Solution. *J. Chem. Phys.* **2006**, *125*, 054103.
(58) Marenich, A.; Cramer, C.; Truhlar, D.; Guido, C.; Mennucci, B.; Scalmani, G.; Frisch, M. Practical Computation of Electronic Excitation in Solution: Vertical Excitation Model. *Chem. Sci.* **2011**, *2*, 2143−2161.
(59) Ponder, J. W. *Tinker, Software Tools for Molecular Design*, 3.8; Washington University School of Medicine: St. Louis, MO, 2000.
(60) Neugebauer, J.; Baerends, E. J.; Nooijen, M.; Autschbach, J. Importance of Vibronic Effects on the Circular Dichroism Spectrum of Dimethyloxirane. *J. Chem. Phys.* **2005**, *122*, 234−305.
(61) Lange, A.; Herbert, J. M. Simple Methods to Reduce Charge-Transfer Contamination in Time-Dependent Density-Functional Calculations of Clusters and Liquids. *J. Chem. Theory Comput.* **2007**, *3*, 1680−1690.
(62) Srebro, M.; Govind, N.; de Jong, W. A.; Autschbach, J. Optical Rotation Calculated with Time-Dependent Density Functional Theory: The OR45 Benchmark. *J. Phys. Chem. A* **2011**, *115*, 10930−10949.
(63) Srebro, M.; Autschbach, J. Tuned Range-Separated Time-Dependent Density Functional Theory Applied to Optical Rotation. *J. Chem. Theory Comput.* **2012**, *8*, 245−256.
(64) Wilson, S. M.; Wiberg, K. B.; Cheeseman, J. R.; Frisch, M. J.; Vaccaro, P. H. Nonresonant Optical Activity of Isolated Organic Molecules. *J. Phys. Chem. A* **2005**, *109*, 11752−11764.
(65) Crawford, T. D.; Stephens, P. J. Comparison of Time-Dependent Density-Functional Theory and Coupled Cluster Theory for the Calculation of the Optical Rotations of Chiral Molecules. *J. Phys. Chem. A* **2008**, *112*, 1339−1345.